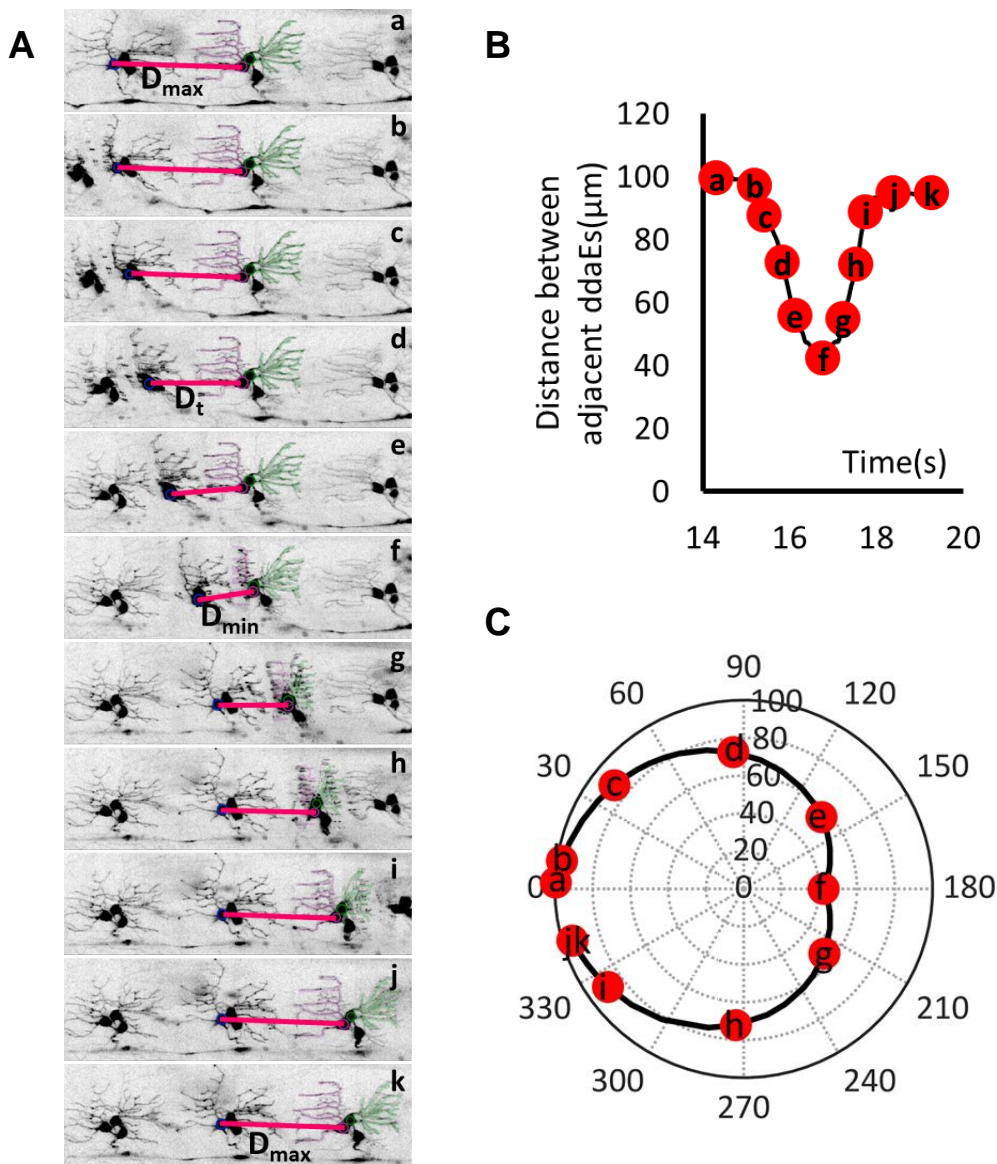


**Figure S1. Movement-related changes in mCD8::GFP signal in wildtype and GCaMP6f signal in *Tmc*<sup>1</sup> mutant. Related to Figures 1 and 2.**

**(A)** Comparison of peak  $\Delta F/F$  in ddaE and ddaD neurons in *Tmc* wildtype expressing mCD8::GFP (n=22) and in *Tmc*<sup>1</sup> mutant expressing GCaMP6f (n=36 (ddaE), n=43 (ddaD)) during forward movement. There is no significant differences in peak  $\Delta F/F$  between ddaE and ddaD for either control (p=0.63) or *Tmc*<sup>1</sup> mutant (p=0.23) in forward movement. ddaE and ddaD in *Tmc*<sup>1</sup> mutant larvae show slightly bigger change in peak fluorescence intensity compared with *Tmc* wildtype in response to larval forward movement. Fluorescence of GFP or GCaMP6f in neurons was imaged from 6 and 10 animals for *Tmc* wildtype and *Tmc*<sup>1</sup> mutant respectively.

**(B)** Comparison of peak  $\Delta F/F$  in ddaE and ddaD neurons in *Tmc* wildtype expressing mCD8::GFP (n=25) and in *Tmc*<sup>1</sup> mutant expressing GCaMP6f (n=35) during backward movement. There is no significant differences in peak  $\Delta F/F$  between ddaE and ddaD for either control (p=0.16) or *Tmc*<sup>1</sup> mutant (p=0.66) in backward movement. ddaE and ddaD in *Tmc*<sup>1</sup> mutant show slightly bigger change in peak fluorescence intensity compared with *Tmc* wildtype in response to backward movement. Fluorescence of GFP or GCaMP6f in neurons was imaged from 7 and 11 animals for *Tmc* wildtype and *Tmc*<sup>1</sup> mutant respectively. These data do not rule out the possibility that a residual physiological response remains in the *Tmc*<sup>1</sup> mutant background.



**Figure S2. Definition of segmental contraction cycle. Related to Figures 1,2,3,5,6 and 7.** **(A)** Real time images shows a segmental contraction cycle. The segmental contraction cycle is defined as the repetitive shortening and lengthening of the distance between the adjacent neuron-pair (ddaE or ddaD) in neighboring segments. A typical cycle starts from when the distance between the neuron-pair is at the maximal distance, reaches minimal, and back to maximal again as depicted in panel **A**. **(B)** Centroid distance between adjacent ddaE neurons was plotted as a function of time. Time for a contraction cycle is different for each movement or larva. **(C)** Centroid distances of neighboring ddaE-pair over time were plotted in phase of a 360 degree cycle. Position along the radial axis represents the distance between adjacent ddaE neurons showed in **A**. The centroid distances of neighboring neuron-pair over time were further converted to the phase angles. For each cycle, maximal distance between neighboring neuron-pair (initiation of the contraction) is set to phase 0, and the minimal distance (initiation of relaxation) is set to phase 180. The end of the cycle is when it reaches the maximal distance (phase 0/360). The formula  $\Theta_{t} = (D_{max} - D_t) * (\pi / (D_{max} - D_{min}))$  was used to convert distance to phase angle coordinate (0 to 180) and  $\Theta_{t} = 2 * \pi - (D_{max} - D_t) * (\pi / (D_{max} - D_{min}))$  was used to convert distance to phase angle coordinate (181 to 360), where  $D_{max}$  is the maximal distance between neuron-pair,  $D_{min}$  is the minimal distance between neuron-pair, and  $D_t$  is the distance between neuron-pair at a given time in the cycle.

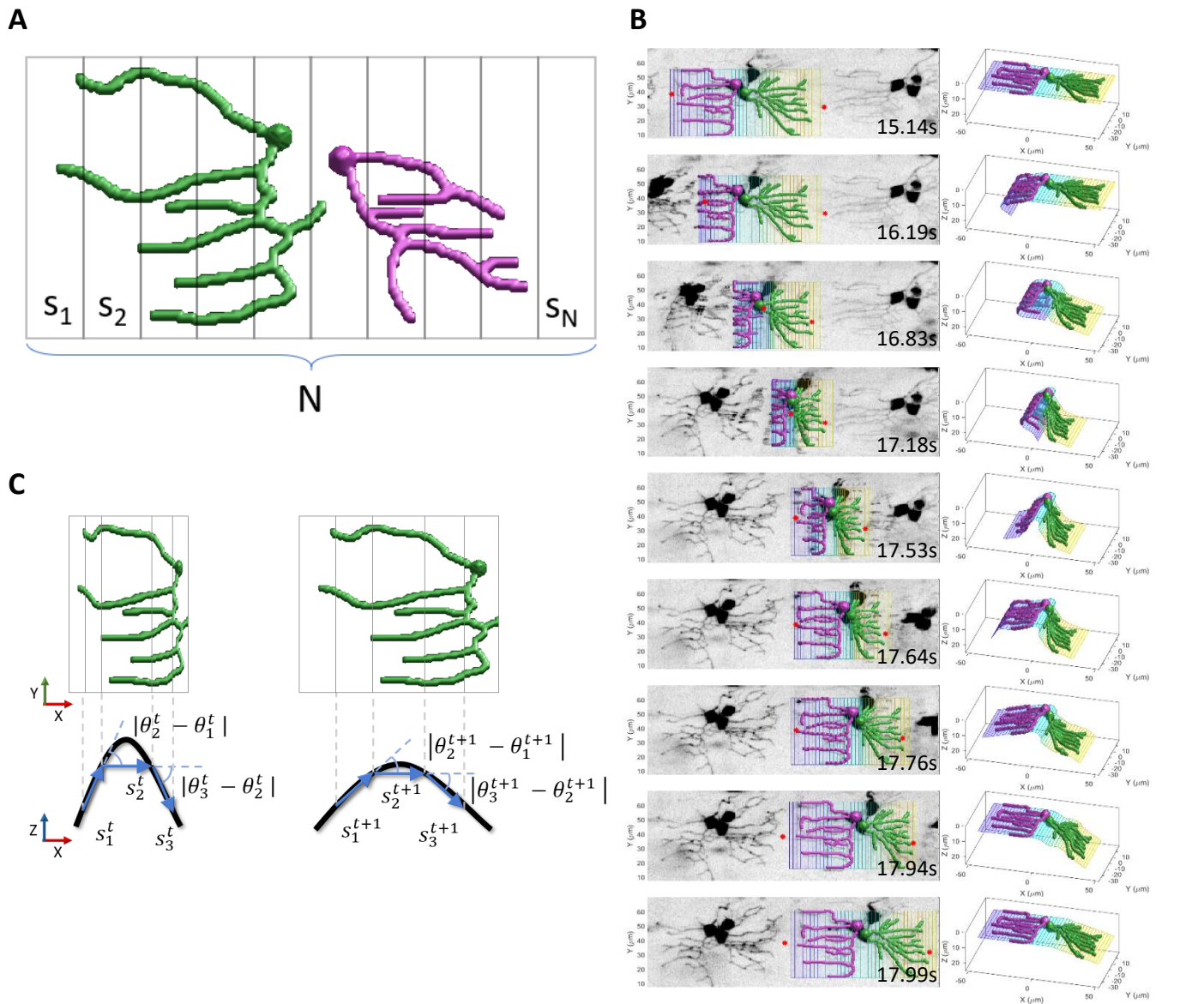
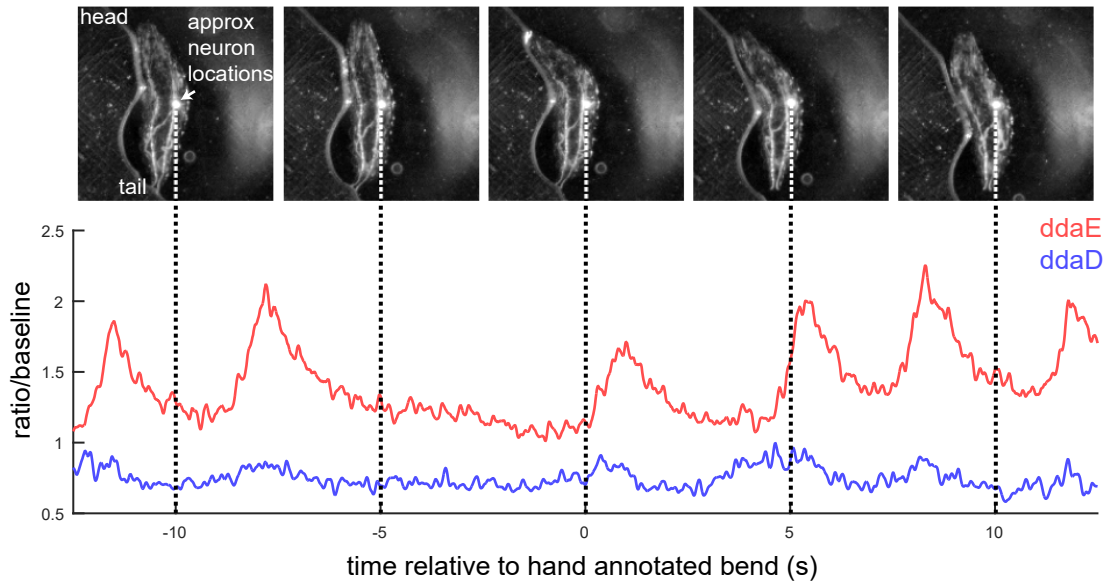


**Figure S3. The accordion model. Related to Figure 5.**

**(A)** The neuron accordion model enclosing the body segment consists of  $N$  strips  $S_1, S_2, S_3, \dots, S_N$ . **(B)** The algorithm requires the X-coordinates of the farthest dendrite tips as shown by red asterisks. ddaD and ddaE neurons are shown in green and magenta colors respectively. The colored strips constitute the neuron accordion model. (Left) the 2D view. (Right) the 3D view. From top to bottom, the neuron accordion model over a contraction cycle — the ground truth dendrites, and the deformed neurons in frames at various time points. Notes: ventral is up and anterior is to the right. **(C)** The dendrite curvature can be approximated using the curvature of the accordion model, which captures the dendrite deformation from the locomotion induced strain. Let  $S^t = \{s_i^t\}$  be the set of  $N$  strips of the accordion model at time  $t$ , for  $i = 1, \dots, N$ . Also let  $\theta^t = \{\theta_i^t\}$  be the configuration of angles formed with the surface of the accordion model, i.e., the orientation in the XZ-plane of the adjacent strips. Using finite differences, we calculate the curvature of the accordion model  $\kappa^t$  as,  $\kappa^t = \sum_{i=1}^{N-1} |\theta_{i+1}^t - \theta_i^t|$ . Both models are the same accordion model with different configurations. The model on the left has the higher curvature than the model on the right so they appear differently in XY-plane (top) and XZ-plane (bottom).

## A contralateral turn during forward crawling



## B ipsilateral turn during forward crawling

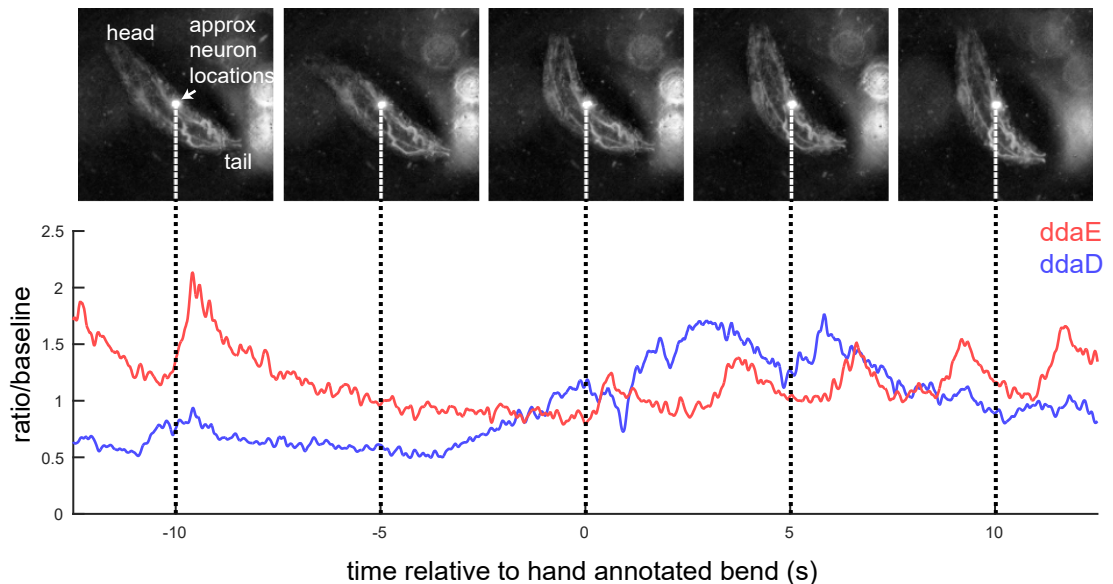


### Figure S4. Representative images of body bends observed under the 2-photon tracking microscope. Related to Figure 4.

The top images in **A** and **B** are still images from video sequences of larval locomotion in the chamber. The bright spot in each panel indicates focal point of the 2-photon laser. The bottom shows the ratiometric traces of neural activity with dashed lines that indicate the time point at which the images have been extracted.

**(A)** Representative contralateral bend in which the larva turns towards the side of the body opposite to the tracked neurons. Note that *ddaD* remains quiescent.

**(B)** Representative ipsilateral bend which shows an increase in *ddaD* activity during the bend.

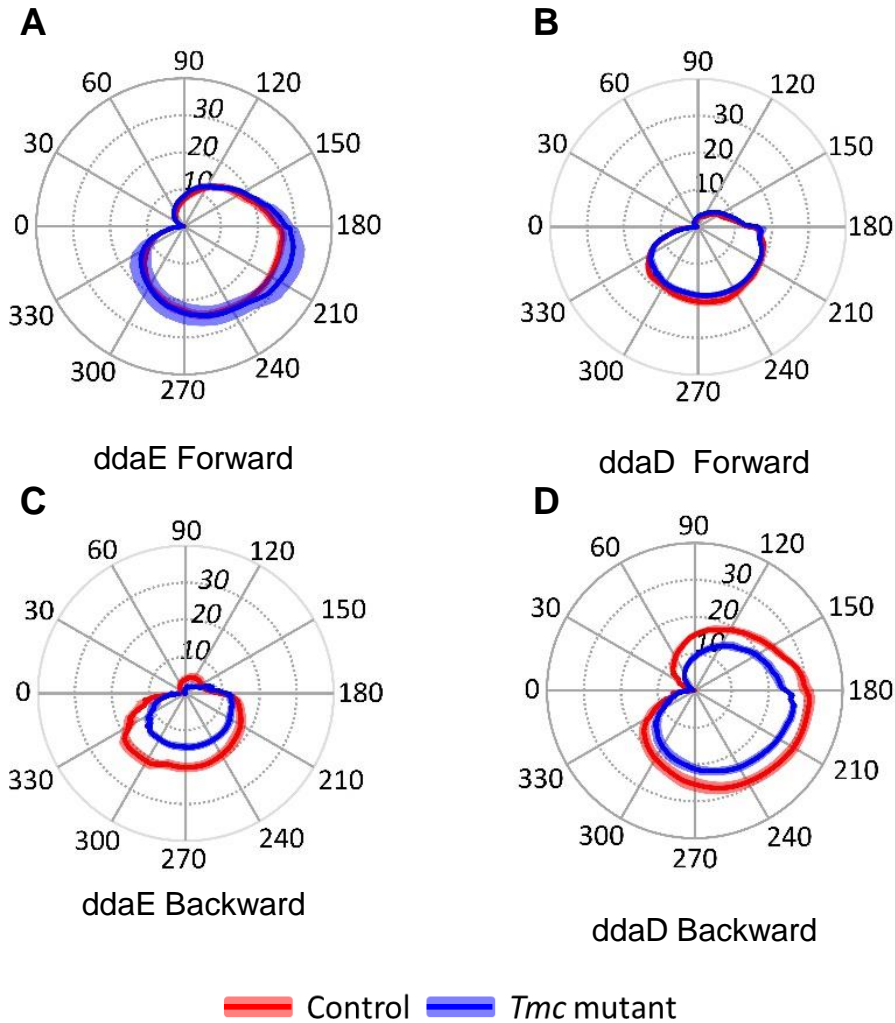


**Figure S5. *Tmc*<sup>1</sup> mutant larvae show similar change in dendrite curvature as *Tmc* wildtype (control) both during forward and backward movement. Related to Figure 7. (A,B) Comparison of dendrite curvature in ddaE(A) and ddaD(B) neurons between *Tmc* wildtype (n=21 from 7 animals) and *Tmc*<sup>1</sup> mutant (n=29 from 14 animals) in larval forward locomotion. (C,D) Comparison of dendrite curvature of ddaE(C) and ddaD(D) neurons between *Tmc* wildtype (n=10 from 6 animals) and *Tmc*<sup>1</sup> mutant (n=13 from 9 animals) in larval backward locomotion.**

Dendrite curvature of ddaE or ddaD neurons plotted versus phase of the segmental contraction cycle. Position along the radial axis represents absolute value of curvature. Solid colored line represents mean of curvature, colored shading represents standard error of mean. n is the number of neurons examined.

<b>all</b>	n bends	p-value comparing ipsi to contra
ddaE ipsi	32	0.61
ddaE contra	33	
ddaD ipsi	29	8.1*10 <sup>-8</sup>
ddaD contra	33	
<b>forward</b>	n bends	p-value comparing ipsi to contra
ddaE ipsi	14	0.70
ddaE contra	19	
ddaD ipsi	9	2.2*10 <sup>-6</sup>
ddaD contra	18	
<b>backward</b>	n bends	p-value comparing ipsi to contra
ddaE ipsi	8	0.27
ddaE contra	7	
ddaD ipsi	12	0.06
ddaD contra	3	
<b>simultaneous recording</b>	n bends	p-value comparing ipsi to contra
ddaE ipsi	11	0.85
ddaE contra	15	
ddaD ipsi	11	8.5*10 <sup>-6</sup>
ddaD contra	15	

**Table S1. Quantification of larval bends during turning behavior. Related to Figure 4.**